Supporting Information

for

The aggregation-enhancing Huntingtin N-terminus is helical in amyloid fibrils.

V.N. Sivanandam[1], Murali Jayaraman[1,2], Cody L. Hoop[1], Ravindra Kodali[1,2], Ronald Wetzel[1,2], and Patrick C.A. van der Wel[1]

[1]Department of Structural Biology, and [2] Pittsburgh Institute for Neurodegenerative Diseases, University of Pittsburgh School of Medicine, Pittsburgh, PA

Table S1 – ^{13}C chemical shift resonances[a].

htt$^{NT}Q_{30}P_{10}K_2$ fibrils							
Res.	**Cα**	**Cβ**	**Cγ**	**Cδ(1)**	**Cδ2**	**Cε**	**CO**
A2	52.7 ±0.26	19.1 ±0.11					178.2 ±0.26
L4	57.8 ±0.10	41.1 ±0.21	27.1 ±0.15	27.1 ±0.2	24.48 ±0.10		178.4 ±0.3
K6	59.5 ±0.10	32.6 ±0.14	25.8 ±0.15	29.55 ±0.10		42.1 ±0.10	179.9 ±0.10
L7	57.8 ±0.19	41.9 ±0.13	26.8 ±0.19	25.2 ±0.11	27.2 ±0.08		178.3 ±0.14
A10	55.0 ±0.19	18.1 ±0.15					180.0 ±0.29
F11[b]	61.2 ±0.3	39.3 ±0.3	131.4 ±0.3				b)
L14	55.7 ±0.36	42.1 ±0.16	26.6 ±0.33	26.6 ±0.33	23.3 ±0.24		177.0 ±0.44
S16	56.8 ±0.3	65.2 ±0.3					173 ±0.5
	58.9 ±0.3	62.8 ±0.3					173 ±0.5
F17[b]	57.1 ±0.10	b)	131.7 ±0.19				175.8 ±0.31
	56.6 ±0.12	b)	131.7 ±0.19				174.3 ±0.23
Q18	55.7 ±0.27	34.2 ±0.16	34.4 ±0.16	178.8 ±0.18			175.6 ±0.10
	54.7 ±0.13	30.85 ±0.14	30.65 ±0.14	177.8 ±0.16			174.2 ±0.14
Q19	56.0 ±0.16	34.2 ±0.15	34.15 ±0.06	178.6 ±0.10			176.0 ±0.16
	53.9 ±0.10	31.1 ±0.42[c]	30.6 ±0.34[c]	177.6 ±0.10			174.2 ±0.10
Pro[d]	61.2 ±0.2	31.9 ±0.2	27.3 ±0.2	50.3 ±0.2			
$K_2Q_{30}K_2$ fibrils							
Res.	**Cα**	**Cβ**	**Cγ**	**Cδ(1)**	**Cδ2**	**Cε**	**CO**
Q6	56.4 ±0.2	34.6 ±0.1	33.9 ±0.3	178.8 ±0.1			176.0 ±0.2
	54.3 ±0.1	31.7 ±0.2	30.3 ±0.1	177.8 ±0.1			174.0 ±0.1

a) The reported chemical shifts are indirectly referenced relative to aqueous DSS.
b) Some of the Phe resonances could not be identified due to overlap and/or low intensities. Listed Cγ resonances reflect the maximum of a broad peak from the combined aromatic resonances (see **Figure S3**).
c) These Q19 peaks sometimes appear as split into two closely spaced cross-peaks.
d) Tentatively assigned resonances of unlabeled Pro. These identifications are based on similarity to typical Pro shifts and the relative abundance of the 10 Pro in the primary sequence. These values are thought to reflect the bulk of the Pro, but specific residues could deviate from these shifts. The observed shift pattern corresponds well to that of previously reported polyPro shifts in a PPII conformation, in the solution as well as solid state [1].

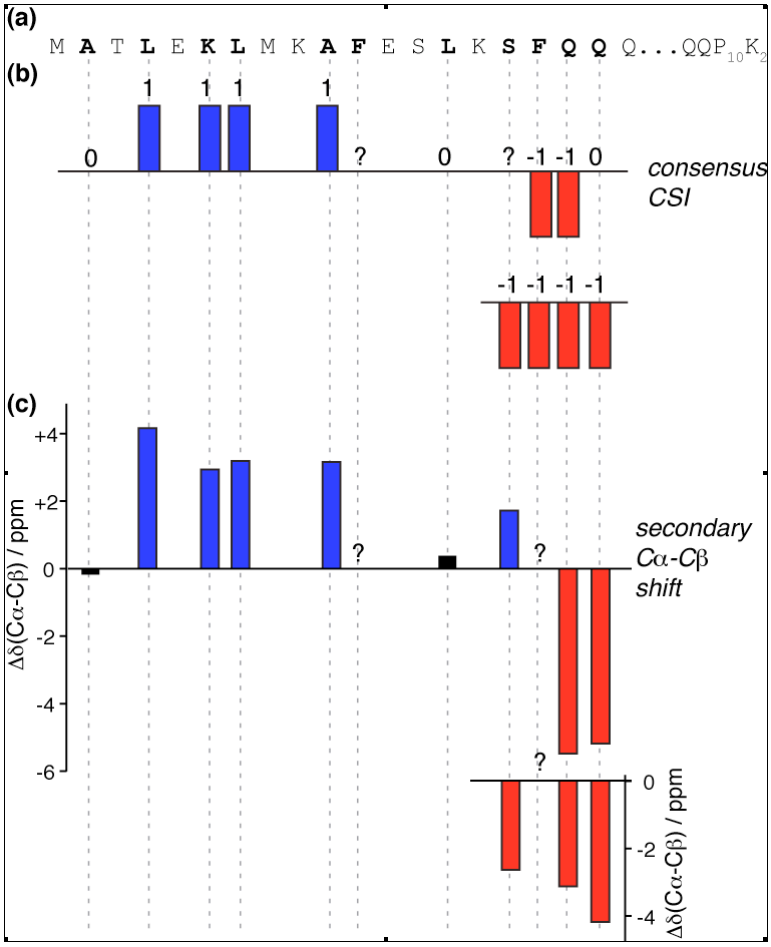

Figure S1 – Secondary structure. (a) Sequence of htt$^{NT}Q_{30}P_{10}K_2$, with labeled sites marked in bold. (b) Graphical representation of consensus CSI for isolated residues[2]. Values of 1, 0, and -1 indicate α-helix, undefined secondary structure and β-sheet, respectively (color coded as in Fig. 5). Question marks indicate sites where the consensus CSI approach was ambivalent (in part due to a few unobserved Phe resonances – see table S1). Doubled resonances are shown as two separate rows, where the grouping is arbitrary and does not indicate that the top and bottom rows are expected to be in the same molecule. (c) Alternative approach to secondary structure analysis based on the characteristic shift difference between the Cα and Cβ sites. This approach benefits from its lack of sensitivity to referencing errors, and has been proposed as particularly useful for ssNMR[3]. Unobserved Phe Cβ sites prevent analysis of these residues and are marked by question marks. Positive and negative values indicate α-helical (blue) and β-sheet backbone conformations (red), respectively.

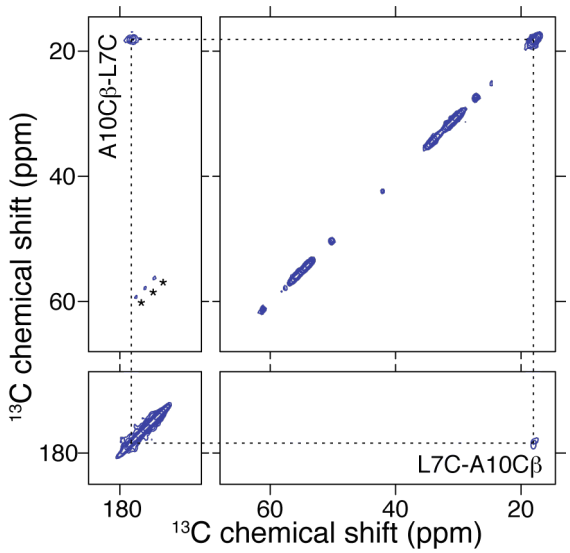

Figure S2 – Observation of L7-A10 inter-residue contact. Inter-residue cross-peaks between A10-Cβ and L7-C' are observed in this 400ms PDSD experiment on sample p4, indicating an *i*-(*i*+*3*) contact. This is consistent with a helical conformation, but not an extended β-sheet. The possibility of inter-molecular interactions contributing to the cross-peak can not be entirely excluded, as the sample was 100% labeled, but seems less likely given the observed significant mobility of the helix.

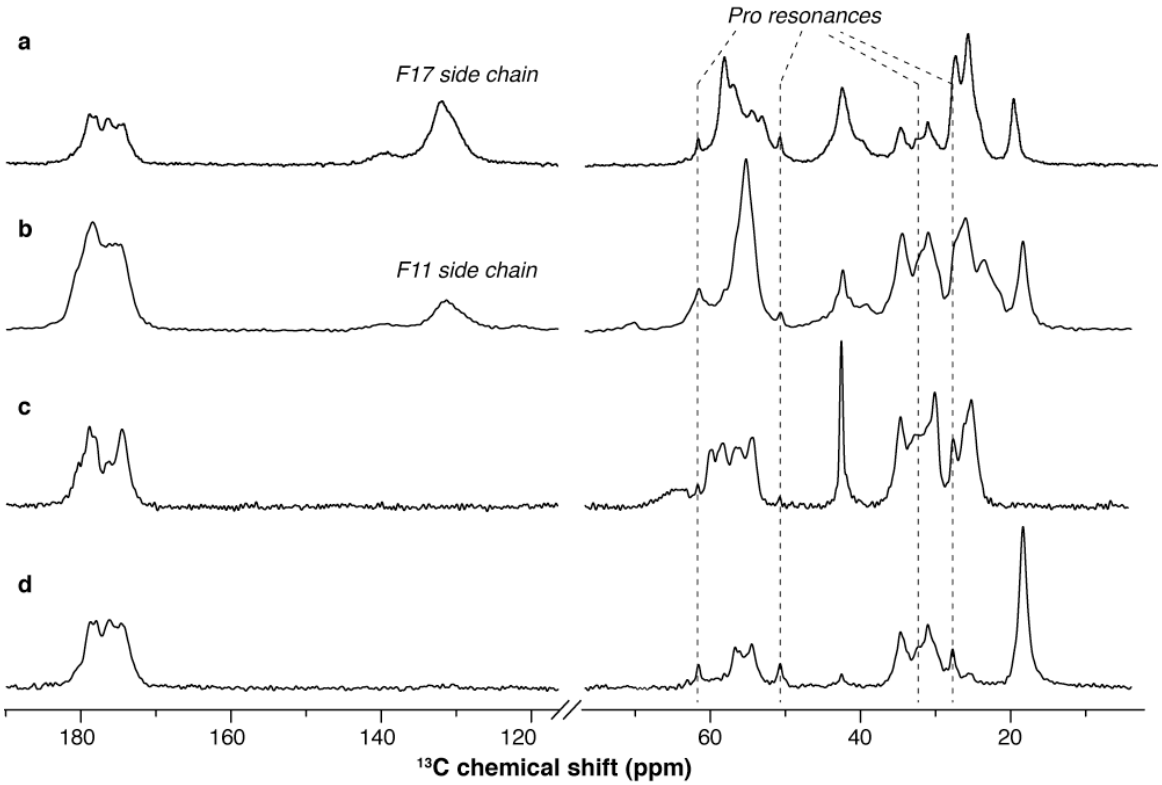

Figure S3 – 1D ^{13}C CP spectra of samples p1 (a), p2 (b), p3 (c), and p4 (d). (a) and (b) include the aromatic signals due to the phenylalanine side chains of F17 and F11. These aromatic signals are severely broadened, a feature that is indicative of motional averaging (e.g. ring flip). The spectra also include background signals due to natural abundance (NA) ^{13}C signals from unlabeled residues, in particular in spectrum (d) where only three carbons are labeled (sample p4: ^{13}C'-L7,^{13}Cβ-A10,^{13}C'-F17). Vertical dashed lines mark the position of NA resonances consistent with Pro sites in a PPII conformation (see also Table S1).

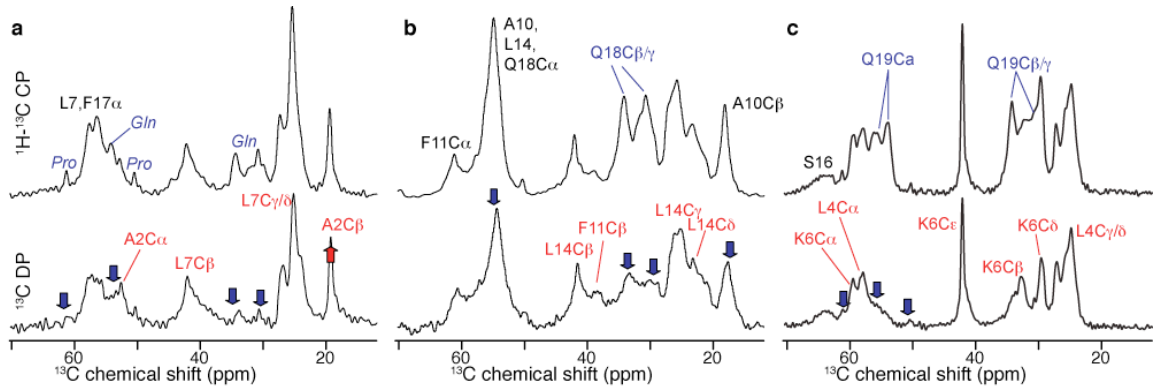

Figure S4 – Site-specific dynamics via motionally sensitive 1D ssNMR. The ^{13}C aliphatic region for the isotopically labeled samples p1 (a), p2 (b) and p3 (c) is shown, from ^{1}H-^{13}C CP spectra (top) and direct excitation ^{13}C spectra (bottom), the latter using relatively short recycle delays. Peaks that are suppressed in the bottom row have a long ^{13}C T_1 and are most rigid (indicated by blue arrows). Peak assignments are color coded, with the most rigid sites in blue, and the more mobile sites in red. NA residue group assignments are indicated in italics. These site-specific differences in mobility provide a more fine-grained picture consistent with the NA ^{13}C spectra. The β-sheet Gln sites are again highly rigid. The mobile signals are located within the htt^{NT} segment and include residues that are helical or lack a defined secondary structure.

Table S2 – Sequences, labeling and amounts of isotopically labeled NMR samples.

ID	Labeling	Sequence[a]	Amount (mg)
p1	U-^{13}C,^{15}N-[A2, L7, F17]	M<u>A</u>TLEK<u>L</u>MKAFESLKS<u>F</u>QQQ-$Q_{27}P_{10}K_2$	2
p2	U-^{13}C,^{15}N-[A10, F11, L14, Q18]	MATLEKLMK<u>AF</u>ES<u>L</u>KSF<u>Q</u>QQ-$Q_{27}P_{10}K_2$	3
p3	U-^{13}C,^{15}N-[L4, K6, S16, Q19]	MAT<u>L</u>E<u>K</u>LMKAFESLK<u>S</u>FQ<u>QQ</u>-$Q_{27}P_{10}K_2$	1.8
p4	^{13}C'-L7,^{13}Cβ-A10,^{13}C'-F17	MATLEK<u>L</u>MK<u>A</u>FESLKS<u>F</u>QQQ-$Q_{27}P_{10}K_2$	5.2
n/a	U-^{13}C,^{15}N-[Q6]	KKQQQ<u>QQ</u>$_{26}$KK	4

a) The labeled residues are also shown as underlined in the primary sequence.

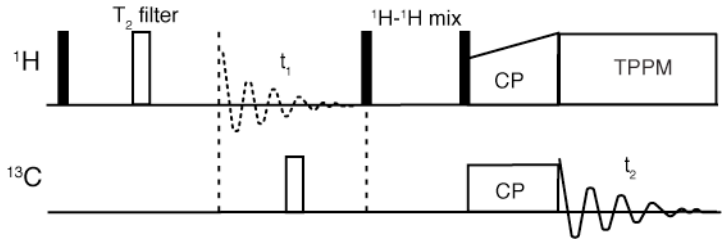

Figure S5 – Water-filtered HETCOR pulse sequence. A T_2 filter is used to eliminate rigid protons, followed by a longitudinal ^{1}H-^{1}H mixing period. The t_1 evolution period is omitted for the 1D spectra (e.g. Figure 7), but allows the unequivocal identification of the source of the proton magnetization in 2D experiments.

Table S3 – Detailed experimental conditions of 1D and 2D NMR experiments shown in the main text and supporting information.

1D spectra[a]									
Figure	Sample[b]	Experiment	NS	Temp. (K)	MAS (kHz)	RD (s)	TPPM during ACQ. (kHz)	T_2 filter time (ms)	^{1}H-^{1}H Mixing (ms)
6	p4	^{1}H-^{13}C CP	1024	275	10	3	83	n/a	n/a
6	p5*	^{1}H-^{13}C CP	2662	275	10	3	83	n/a	n/a
6	p5*	^{13}C 1D	2048	275	12	3	83	n/a	n/a
6	$K_2Q_{31}K_2$*	^{1}H-^{13}C CP	2560	275	10	3	83	n/a	n/a
6	$K_2Q_{31}K_2$*	^{13}C 1D	2048	275	10	3	83	n/a	n/a
6	$K_2Q_{30}K_2$	^{13}C 1D	2048	275	10	3	83	n/a	n/a
7	p2	^{1}H-^{13}C CP	512	275	12	3.5	83	n/a	n/a
7	p3	^{1}H-^{13}C CP	512	275	12	3.5	83	n/a	n/a
7	p2	^{1}H t_2 filter	4096	275	12	3.5	83	1.0	0
7	p3	^{1}H t_2 filter	4096	275	12	3.5	83	1.0	0
7	p2	^{1}H t_2 filter	4096	275	12	3.5	83	1.0	7
7	p3	^{1}H t_2 filter	4096	275	12	3.5	83	1.0	7
S3, S4	p1	^{1}H-^{13}C CP	2048	267	16	4	83	n/a	n/a
S3, S4	p2	^{1}H-^{13}C CP	8192	273	10	4	83	n/a	n/a
S3, S4	p3	^{1}H-^{13}C CP	2048	275	13	3.5	83	n/a	n/a
S4	p1	^{13}C 1D	2048	267	16	3	83	n/a	n/a
S4	p2	^{13}C 1D	2048	273	10	3	83	n/a	n/a
S4	p3	^{13}C 1D	4096	275	13	3.5	83	n/a	n/a
2D spectra[a]									
Figure	Sample	Experiment	NS	Temp. (K)	MAS (kHz)	RD (s)	TPPM during t_1/ACQ (kHz)	t_1 evol. (μs)	Mixing (ms)
3a	p1	DARR 2D	64	267	16	3.5	83	480x20.83	25
3b, 4a	p2	DARR 2D	32	273	10	3.5	83	550x22.07	25
3c, 4b	p3	DARR 2D	96	275	13	3	83	832x19.23	25
4c	$K_2Q_{30}K_2$	DARR 2D	96	275	10	3	83	550x22.07	25
4d	p3	$SPC5_3$ 2D	1152	275	12	3	83	64x100	1.5
S2	p4	PDSD 2D	64	275	12	3	83	290x66.67	400

a) Abbreviations used are: NS: number of scans per t_1 point; RD: recycle delay; Temp.: temperature of cooling gas; TPPM: ^{1}H decoupling during t_1 evolution or acquisition periods.
b) Unlabeled samples are indicated with an asterisk (*).

References cited in the supporting information

(1) Kricheldorf, H.; Müller, D. *Int. J. Biol. Macromol.* **1984**, *6*, 145-151.
(2) Wishart, D. S.; Sykes, B. D. *J. Biomol. NMR* **1994**, *4*, 171-80.
(3) Luca, S.; Filippov, D. V.; van Boom, J. H.; Oschkinat, H.; de Groot, H. J. M.; Baldus, M. *J. Biomol. NMR* **2001**, *20*, 325-31.